Artificial Intelligence 318 (2023) 103898

Contents lists available at ScienceDirect

Artificial Intelligence

journal homepage: www.elsevier.com/locate/artint

On approximating shortest paths in weighted triangular tessellations ☆

Prosenjit Bose [a], Guillermo Esteban [a,b,*], David Orden [b], Rodrigo I. Silveira [c]

[a] Carleton University, Ottawa, Canada
[b] Universidad de Alcalá, Alcalá de Henares, Spain
[c] Universitat Politècnica de Catalunya, Barcelona, Spain

ARTICLE INFO

Article history:
Received 9 April 2022
Received in revised form 22 February 2023
Accepted 25 February 2023
Available online 5 March 2023

Keywords:
Shortest path
Any-angle path planning
Tessellation
Weighted region problem

ABSTRACT

We study the quality of weighted shortest paths when a continuous 2-dimensional space is discretized by a weighted triangular tessellation. In order to evaluate how well the tessellation approximates the 2-dimensional space, we study three types of shortest paths: a weighted shortest path $SP_w(s,t)$, which is a shortest path from s to t in the space; a weighted shortest vertex path $SVP_w(s,t)$, which is an any-angle shortest path; and a weighted shortest grid path $SGP_w(s,t)$, which is a shortest path whose edges are edges of the tessellation. Given any arbitrary weight assignment to the faces of a triangular tessellation, thus extending recent results by Bailey et al. (2021) [6], we prove upper and lower bounds on the ratios $\frac{\|SGP_w(s,t)\|}{\|SP_w(s,t)\|}$, $\frac{\|SVP_w(s,t)\|}{\|SP_w(s,t)\|}$, $\frac{\|SGP_w(s,t)\|}{\|SVP_w(s,t)\|}$, which provide estimates on the quality of the approximation. It turns out, surprisingly, that our worst-case bounds are independent of any weight assignment. Our main result is that $\frac{\|SGP_w(s,t)\|}{\|SP_w(s,t)\|} = \frac{2}{\sqrt{3}} \approx 1.15$ in the worst case, and this is tight. As a corollary, for the weighted any-angle path $SVP_w(s,t)$ we obtain the approximation result $\frac{\|SVP_w(s,t)\|}{\|SP_w(s,t)\|} \lessapprox 1.15$.

1. Introduction

Geometric shortest path problems, where the goal is to find an optimal path between two points s and t in a geometric setting, are fundamental for variety of real-world applications. For example, autonomous navigation over different types of terrain is a building block of an intelligent vehicle [29,42,47]. Artificial intelligence is also an important part in the design of video games [25,43]; developers usually design the movement of non-player characters following the edges of the cells that decompose the space. See Fig. 1, which shows how 2D triangular cells are used in the strategy game "Colossal Citadels" [28]. Moreover, finding paths of minimum cost is one of the major features in geographic information science [17].

One of the most general settings for geometric shortest path problems arises when the cost of traversing the plane varies depending on the region, that is, when the domain consists of a planar subdivision and each region i of the subdivision has a weight ω_i, that represents the cost per unit of distance traveled in that region.

In gaming applications, this can be seen as an agent moving at different speeds when traversing a road, a dirt track, a forest, or a swamp area. Infrastructure planning takes into consideration planning, ecological and economic decision criteria.

☆ This is an extended version of a paper appearing in Proceedings of WALCOM 2022.

* Corresponding author at: Universidad de Alcalá, Alcalá de Henares, Spain.
E-mail addresses: jit@scs.carleton.ca (P. Bose), g.esteban@uah.es (G. Esteban), david.orden@uah.es (D. Orden), rodrigo.silveira@upc.edu (R.I. Silveira).

https://doi.org/10.1016/j.artint.2023.103898

Fig. 1. Screenshots of the "Colossal Citadels" game by Uneven Dungeon. Used with permission from the author. Note the triangular grid underlying the scene.

Hence, finding proper weights on a raster-based accumulated cost surface is crucial when placing power lines [5,21], and pylons [36,39]. It is also fundamental in the construction of highways and corridors [40]. Thus, the cost of traversing a region is typically given by the Euclidean distance traversed in the region, multiplied by the corresponding weight. The resulting metric is often called the *weighted region metric*, and the problem of computing a shortest path between two points under this metric is known as the *weighted region problem* (WRP) [30,31].

1.1. Assumptions

Applications usually require efficient and practical solutions for the WRP. Since an exact solution to the WRP is notoriously difficult, the problem is usually simplified in two ways. First, the domain is approximated by using a (weighted) plane subdivision with a simpler structure. Secondly, optimal shortest paths in that simpler subdivision are approximated. The typical way to represent a 2D (or 3D) environment where shortest paths need to be computed is by using *navigational meshes* [46]. These are polygonal subdivisions together with a graph that models the adjacency between the regions. Path planning is then done first on the graph, to obtain a sequence of regions to be traversed, and then within each region, for which a shortest geometric path is extracted.

Triangles, convex polygons, disks or squares —of different sizes— are among the most frequently used region shapes [46]. General navigational meshes allow efficient path planning in large environments as long as the region weights are limited to $\{1, \infty\}$ (i.e., free movement or obstacles), but when more weights $\{1, \omega_i, \ldots, \omega_j, \infty\}$ are needed (i.e., modeling different speeds for different types of ground), the complexity of computing the shortest path inside each region is most easily achieved through the use of the simplest possible navigational mesh: *regular grids*.

In 2D, the only three types of regular polygons that can be used to tessellate continuous environments are triangles, squares and hexagons. The drawback with a grid is that it imposes a fixed resolution, requiring in general a large number of cells or regions. Still, grids are often used as navigational meshes (even for the simpler case of weights $\{1, \infty\}$), since they are easy to implement, are a natural choice for environments that are grid-based by design (e.g., many game designs, some robotic settings), and popular shortest path algorithms such as A^* can be optimized for grids [22,32,34].

1.2. Definitions and notations

Even when a regular grid is used as a navigational mesh, in practice, computing an exact weighted shortest path $SP_w(s,t)$ is difficult and, in fact, no exact algorithm exists for the WRP [16]: instead, in practice, one usually resorts to approximations, by computing shortest paths on a weighted graph associated to the grid [1–3,14].

To this end, two different graphs have been considered in the literature [6,27,33,34], the *corner-vertex graph* G_{corner} and the *k-corner grid graph* $G_{k\text{corner}}$.

In G_{corner}, the vertex set is the set of corners of the tessellation and every pair of vertices is connected by an edge. This graph is the complete graph over the set of vertices. Fig. 2a depicts some of the neighbors of a vertex v in the corner-vertex graph. Note that in this graph some edges overlap. A path in this graph is called a *vertex path* or *any-angle path*; a shortest vertex path between s and t will be denoted by $SVP_w(s,t)$, where the subscript w highlights that this path depends on a particular weight assignment w.

In $G_{k\text{corner}}$, which is a subgraph of a corner-vertex graph, the vertex set is the set of corners of the tessellation, and each vertex is connected by an edge to a predefined set of k neighboring vertices, depending on the tessellation and other design decisions. See Fig. 2b for the 6-corner grid graph in a triangular tessellation. (Analogous k-corner grid graphs can be defined for square and hexagonal tessellations.) A path in this graph is called a *grid path*; a shortest grid path between s and t will be denoted by $SGP_w(s,t)$.

In all cases, the weight of each graph edge is defined by a function of the weights of the regions that the line segment associated with the edge traverses. More formally, let T_i be a region in a subdivision with weight $\omega_i \in \mathbb{R}_{\geq 0}$. The cost of a segment π in the interior of a cell T_i is given by $\omega_i \|\pi\|$, where $\|\cdot\|$ is the Euclidean norm. In the case where π lies on

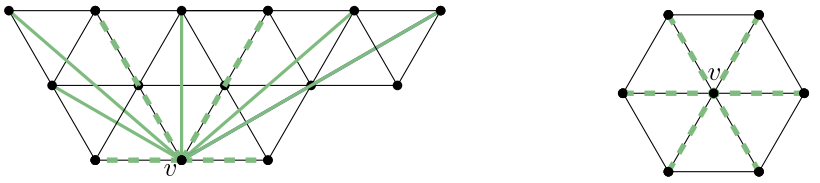

(a) Some neighbors of a vertex v in G_{corner}. (b) All neighbors of a vertex v in $G_{6\text{corner}}$.

Fig. 2. Vertex v is connected to its neighbors in a triangular tessellation. The dashed lines represent the edges of the graphs that coincide with the edges of the cells. (For interpretation of the colors in the figure(s), the reader is referred to the web version of this article.)

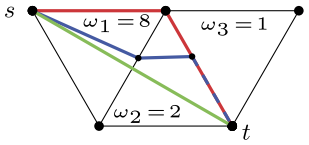

Fig. 3. $SP_w(s,t)$ (blue), $SVP_w(s,t)$ (green), and a $SGP_w(s,t)$ (red) between two corners s and t in $G_{6\text{corner}}$. The cost of each path is 16.75, 17.32 and 18, respectively, for a cell side length of 2.

the boundary of two cells T_j and T_k, the cost is $\min\{\omega_j, \omega_k\}\|\pi\|$. Thus, the weighted length of a path Π is the sum of the weighted lengths of its subpaths through each face and along each edge. With a slight abuse of notation, we still denote this by $\|\Pi\|$.

Fig. 3 shows an example, illustrating the three paths considered in this work: the shortest path $SP_w(s,t)$ (blue), the shortest vertex path $SVP_w(s,t)$ (green), and the shortest grid path $SGP_w(s,t)$ (red) in a 6-corner grid graph. Note that, in the remainder of this work, any cell that is not depicted in the figures is considered to have infinite weight. In addition, if two paths coincide in a segment, one of them is depicted with dashed lines in that segment.

1.3. Quality bounds for approximation paths

The goal of this work is to understand the relation between $SGP_w(s,t)$, $SVP_w(s,t)$, and $SP_w(s,t)$, when a general weight assignment $\{1, \omega_i, \ldots, \omega_j, \infty\}$ is given in the WRP. Since $SVP_w(s,t)$ and $SGP_w(s,t)$ are approximations of $SP_w(s,t)$, a fundamental question is: what is the worst-case approximation factor that they can give?

In particular, we are interested in upper-bounding the ratios $\frac{\|SGP_w(s,t)\|}{\|SP_w(s,t)\|}$ and $\frac{\|SVP_w(s,t)\|}{\|SP_w(s,t)\|}$, since they indicate the approximation factor of the shortest grid path and shortest vertex path, respectively. The ratio $\frac{\|SGP_w(s,t)\|}{\|SVP_w(s,t)\|}$ is also studied, to see how different the two approximations can be.

The major contribution of this paper is the analysis of the quality of the three types of shortest paths for a weighted triangular grid for $G_{6\text{corner}}$, which is the most natural graph defined on a triangular grid.

1.4. Significance

The WRP is very general, since it can be used to model many well-known variants of geometric shortest path problems. Indeed, having all equal weights makes the metric equivalent to the Euclidean metric (up to scaling), while using weights $\{1, \infty\}$ allows to model paths amidst obstacles.

In the latter case, $SGP_w(s,t)$ and $SP_w(s,t)$ have been previously studied (note that $SVP_w(s,t)$ and $SP_w(s,t)$ coincide when the weights of the cells are taken in the set $\{1, \infty\}$). Algorithms using Snell's law of refraction, heuristic methods, or Dijkstra's algorithm are often used to find the shortest grid path [33,44] between two given points. In case of large-scale grid environments some relaxed versions of Dijkstra and A^* with linear running time $O(n)$ (n is the size of the grid) have been designed [4]. Furthermore, some heuristics have been proposed for computing shortest paths in the context of game-programming [33,48], and for mobile robots [11,18,35]. Other algorithms have been suggested for isoline-based world representations [19], or for robots with two degrees of freedom [41]. In addition, some algorithms using heuristics, like Field D*, have been generalized to 3D environments [10] when computing $SP_w(s,t)$.

Almost all previous bounds on the ratio $\frac{\|SGP_w(s,t)\|}{\|SP_w(s,t)\|}$ consider a limited set of weights for the cells. Bailey et al. [6] considered only weights in the set $\{1, \infty\}$ and proved that the weighted length of $SGP_w(s,t)$ in hexagonal $G_{6\text{corner}}$ and $G_{12\text{corner}}$, square $G_{4\text{corner}}$ and $G_{8\text{corner}}$, and triangle $G_{6\text{corner}}$ can be up to ≈ 1.15, ≈ 1.04, ≈ 1.41, ≈ 1.08, and ≈ 1.15 times the weighted length of $SP_w(s,t)$, respectively. In addition, for extended square grid neighborhoods such as $G_{2^k\text{corner}}$ r-constrained it is proved that the length of an r-constrained path is at most $\frac{1}{\cos\left(\frac{\text{arccot}(r)}{2}\right)}$ times the length of a shortest path [23]. For $G_{2^k\text{corner}}$ and $G_{2^k\text{center}}$ [27], theoretical bounds for the ratio $\frac{\|SGP_w(s,t)\|}{\|SP_w(s,t)\|}$ were presented, but no improvement was obtained over the results in [7].

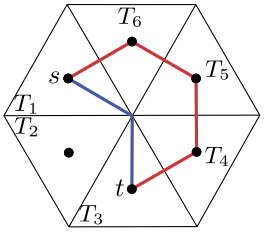

(a) By setting the weight of T_2 to infinity, $SGP_w(s,t)$ (red) must intersect some cells that $SP_w(s,t)$ (blue) does not intersect.

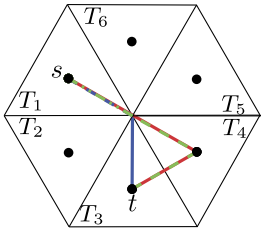

(b) Even if we increase the number of neighbors of each vertex, $SGP_w(s,t)$ (red) and $SVP_w(s,t)$ (green) intersect a cell that $SP_w(s,t)$ (blue) does not intersect. Observe that the three paths coincide from s to the common vertex to T_1 and T_4.

Fig. 4. When the centers of the cells are used as the vertices of the associated graph, we can make the ratios $\frac{\|SGP_w(s,t)\|}{\|SP_w(s,t)\|}$, $\frac{\|SVP_w(s,t)\|}{\|SP_w(s,t)\|}$ arbitrarily large by giving cells T_4, T_5, T_6 a finite weight much greater than 1, and cells T_1, T_3 weight 1.

Perhaps not surprisingly, the WRP turns out to be a challenging problem, so the main challenge here is to obtain tight upper bounds that hold for *any* assignment $\{1, \omega_i, \ldots, \omega_j, \infty\}$ of region weights. Efficient algorithms for the WRP only exist for a few special cases, e.g., rectilinear subdivisions with the L_1 metric [13], or the *maximum concealment problem*, where just regions with weights 0 (travel in concealed free space), 1 (travel in exposed free space), or ∞ (travel through obstacles) are allowed [20,30,31]. This latter version of the WRP is related to stealth video games, such as "Metal Gear" [26] or "Assassin's Creed" [45], where the player uses stealth to avoid or overcome opponents, i.e., the objective is to minimize the time the moving agent is exposed to a given set of "enemy" observers.

The first algorithm for the WRP was a $(1+\varepsilon)$-approximation proposed by Mitchell and Papadimitriou [31], which runs in time $O(n^8 \log(\frac{nNW}{w\varepsilon}))$, where N is the maximum integer coordinate of any vertex of the subdivision, W and w are the maximum finite and the minimum nonzero integer weights assigned to the regions, respectively. Substantial research has been devoted to designing faster approximation algorithms and studying different variants of the problem [1–3,38]. Approximation schemes for the WRP are sophisticated methods that usually are based on variants of the continuous Dijkstra's algorithm, subdividing triangle edges in parts for which crossing shortest paths have the same combinatorial structure (e.g., [31]), or work by computing a discretization of the domain by carefully placing Steiner points (e.g., see [14] for the currently best method of this type). The lack of exact algorithms for the WRP is probably explained by the fact that it was recently shown to be impossible to solve this problem in the Algebraic Computation Model over the Rational Numbers [16]. This is a model of computation where one can compute exactly any number that can be obtained from rational numbers by a finite number of basic operations.

1.5. Results

In this work, we consider tessellations where every face is an equilateral triangle (analogous ideas apply to square and hexagonal grids), and any arrangement of (non-negative) weights $\{1, \omega_i, \ldots, \omega_j, \infty\}$ to the cells of the discrete 2D environment. This extends recent results by Bailey et al. [6], who just considered weights in $\{1, \infty\}$.

Some advantages of triangular grids are that they can include hexagonal grids, and the distance between the vertices of adjacent cells is always the same, which simplifies distance calculations. In terms of computer games, movement of units in tight formation is allowed to have six directions and to turn smoothly. Furthermore, triangles can represent complex shapes, which is useful for building fortresses, bastions and streets, and interesting symmetrical shapes can be used for spells [28].

In contrast to previous work [6,23,27], we allow the weights ω_i to take any value in $\mathbb{R}_{\geq 0}$. When the weights of the cells are allowed to be arbitrary non-negative numbers, the only result that we are aware of is for square tessellations and another type of shortest path, with vertices at the center of the cells, for which Jaklin [24] showed that $\frac{\|SGP_w(s,t)\|}{\|SP_w(s,t)\|} \leq 2\sqrt{2}$. This latter model, considering vertices placed at the centers of the cells, simplifies collision avoidance during path execution, and has produced slightly different approximation results for the 2-dimensional terrain case, see [7] for unweighted square tessellations. However, we do not study the ratios in this model since all of them are unbounded when we assign non-negative weights to the cells, see for instance Fig. 4.

Our main result is that $\frac{\|SGP_w(s,t)\|}{\|SP_w(s,t)\|} = \frac{2}{\sqrt{3}}$ in the worst case, for any (non-negative) weight assignment. This implies bounds for the other two ratios considered. Moreover, our upper bound for $\frac{\|SGP_w(s,t)\|}{\|SP_w(s,t)\|}$ is tight, since it matches the lower bound of Nash [33]. Table 1 summarizes our results, including Nash's lower bounds.

In order to obtain bounds on the ratios, we uncover some properties of the different paths that allow us to prove our approximation ratios. These properties are related to the behavior of shortest paths and to the geometry of a constant number of cells of the tessellation. Surprisingly, a consequence of our analysis is that the worst-case ratios are upper-bounded by constants that are independent of the weights assigned to the regions in the tessellation, i.e., the assignment of arbitrary weights to the cells is not the determining factor on the worst-case ratio.

Table 1
Bounds on the quality of approximations of shortest paths in weighted triangular tessellations for $G_{6\text{corner}}$.

	Lower bound	Upper bound
$\frac{\|SGP_w(s,t)\|}{\|SP_w(s,t)\|}$	$\frac{2}{\sqrt{3}} \approx 1.15$ [33]	$\frac{2}{\sqrt{3}} \approx 1.15$ (Theorem 1)
$\frac{\|SVP_w(s,t)\|}{\|SP_w(s,t)\|}$	$\frac{2\sqrt{7\sqrt{3}-12}}{(7-4\sqrt{3})(6\sqrt{2}+\sqrt{7\sqrt{3}-12})} \approx 1.11$ (Obs. 3)	$\frac{2}{\sqrt{3}} \approx 1.15$ (Corollary 2)
$\frac{\|SGP_w(s,t)\|}{\|SVP_w(s,t)\|}$	$\frac{2}{\sqrt{3}} \approx 1.15$ [33]	$\frac{2}{\sqrt{3}} \approx 1.15$ (Corollary 1)

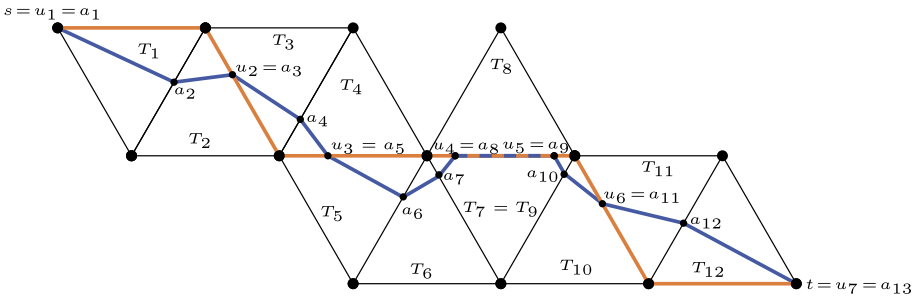

Fig. 5. Weighted shortest path $SP_w(s,t)$ (blue) and the crossing path $X(s,t)$ (orange) from s to t in a triangular tessellation.

2. $\frac{\|SGP_w(s,t)\|}{\|SP_w(s,t)\|}$ ratio in $G_{6\text{corner}}$ for triangular cells

This section is devoted to obtaining, for two vertices s and t, an upper bound on the ratio $\frac{\|SGP_w(s,t)\|}{\|SP_w(s,t)\|}$ in $G_{6\text{corner}}$ in a triangular tessellation $\mathcal{T}$ where faces are assigned arbitrary weights in $\mathbb{R}_{\geq 0}$. We assume that $SP_w(s,t)$ is unique, otherwise it is enough to repeat the following argument where we compute an upper bound for $\frac{\|SGP_w(s,t)\|}{\|SP_w(s,t)\|}$. In addition, we suppose, without loss of generality, that the length of each edge of the triangular cells is 2, in order to have a non-fractional length ($\sqrt{3}$) for the cell height.

Let $(s = u_1, u_2, \ldots, u_\ell = t)$ be the ordered sequence of consecutive points where a grid path $GP_w(s,t)$ and the shortest path $SP_w(s,t)$ coincide; in the case where $GP_w(s,t)$ and $SP_w(s,t)$ share one or more segments, we define the corresponding points as the endpoints of each of these segments, see Fig. 5 for an illustration. Observation 1 below is a special case of the mediant inequality.

Observation 1. *Let $GP_w(s,t)$ and $SP_w(s,t)$ be, respectively, a weighted grid path, and a weighted shortest path, from s to t. Let u_i and u_{i+1} be two consecutive points where $GP_w(s,t)$ and $SP_w(s,t)$ coincide. Then, the ratio $\frac{\|GP_w(s,t)\|}{\|SP_w(s,t)\|}$ is at most the maximum of all ratios $\frac{\|GP_w(u_i,u_{i+1})\|}{\|SP_w(u_i,u_{i+1})\|}$, $i \in \{1, \ldots, \ell - 1\}$.*

2.1. Crossing paths and weakly simple polygons

The shape of the shortest paths $SP_w(s,t)$ and $SGP_w(s,t)$ is unknown to us. Moreover, knowing the exact shape of $SP_w(s,t)$ is difficult. In addition, the two paths might intersect many different cells of the tessellation, so we need to take into account the weights of all the intersected regions. To address all these issues, for a given $SP_w(s,t)$ we define a particular grid path called a *crossing path* $X(s,t)$, whose structure is simpler than the structure of a $SGP_w(s,t)$, and whose weighted length provides an upper bound on the weighted length of $SGP_w(s,t)$. See the orange path in Fig. 5. Thus, since $\|SGP_w(s,t)\| \leq \|X(s,t)\|$, the key idea to prove an upper bound on the ratio $\frac{\|SGP_w(s,t)\|}{\|SP_w(s,t)\|}$ is to upper-bound the ratio $\frac{\|X(s,t)\|}{\|SP_w(s,t)\|}$. To do so, we analyze the components resulting from the intersection between $SP_w(s,t)$ and $X(s,t)$. Each component is a weakly simple polygon, whose boundary consists of the portions of $SP_w(s,t)$ and $X(s,t)$ between the intersection points. The reason the polygons are weakly simple is because some portion of the boundary may be shared between the two paths. These weakly simple polygons are the basic unit that we will analyze to obtain our main result. We also obtain a relation between the weights of some cells intersected by $SP_w(s,t)$ and $X(s,t)$. Notice that, for one type of weakly simple polygon, we will need a finer analysis using *shortcut paths* $\Pi_i(s,t)$, which are defined in Section 2.2 (see Definition 3).

We begin by defining $X(s,t)$. Let $(T_1, \ldots, T_n)$ be the ordered sequence of consecutive triangular cells intersected by $SP_w(s,t)$ in the tessellation $\mathcal{T}$. Let v_1^i, v_2^i, v_3^i be the three consecutive corners on the boundary of T_i, $1 \leq i \leq n$, in clockwise order. Let $(s = a_1, a_2, \ldots, a_{n+1} = t)$ be the sequence of consecutive points where $SP_w(s,t)$ changes the cell(s) it belongs to in $\mathcal{T}$. In particular, let a_i and a_{i+1} be, respectively, the points where $SP_w(s,t)$ enters and leaves T_i. Informally, we define $X(s,t)$ based on $SP_w(s,t)$. Essentially, $SP_w(s,t)$ must traverse a number of cells of the tessellation. Although we

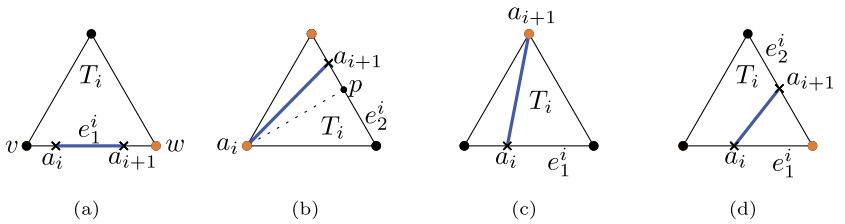

Fig. 6. Some of the positions of the intersection points between $SP_w(s,t)$ (blue) and a cell. The vertices of the crossing path $X(s,t)$ in a triangular cell are depicted in orange.

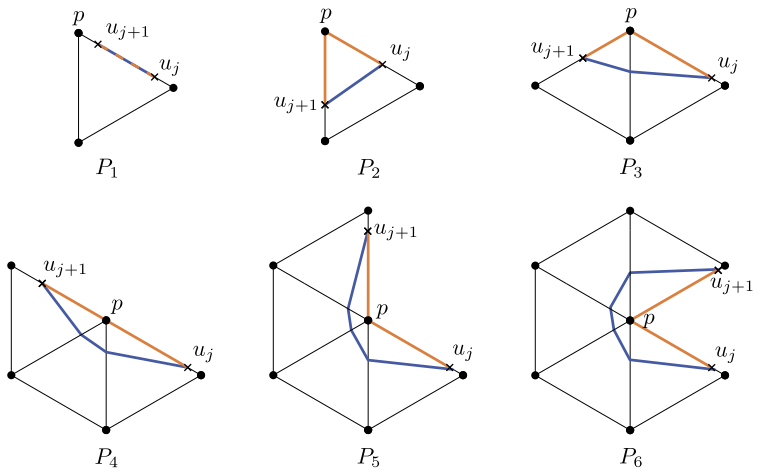

Fig. 7. An example of weakly simple polygon for each type P_k (notice that, w.l.o.g., u_j and u_{j+1} could have other positions), and the subpath of the crossing path $X(s,t)$ (orange) from u_j to u_{j+1} intersecting consecutive triangular cells. $SP_w(u_j,u_{j+1})$ is depicted in blue.

do not know which cells are crossed, based on the geometry of the cell, we can compute an approximate path, $X(s,t)$. We formalize this notion below:

Definition 1. The *crossing path* $X(s,t)$ between two vertices s and t is defined by the sequence $(X_1,\ldots,X_n)$, where X_i is a sequence of vertices determined by the pair (a_i,a_{i+1}), $1\le i\le n$, as follows:

1. If a_i and a_{i+1} are on the same edge $e_1^i\in T_i$, let v and w be the endpoints of e_1^i, where a_i is encountered before a_{i+1} when traversing e_1^i from v to w. Then $X_i=(v,w)$ if $a_i=v$, and $X_i=(w)$ otherwise, see Fig. 6a.
2. If a_i is a corner of T_i, and a_{i+1} belongs to the interior of the edge $e_2^i\in T_i$ not adjacent to a_i, let p be the midpoint of e_2^i. If a_{i+1} is to the left of $\overrightarrow{a_ip}$, X_i is a_i and the endpoint of e_2^i to the left of $\overrightarrow{a_ip}$, see Fig. 6b. Otherwise, X_i is a_i and the endpoint of e_2^i to the right of $\overrightarrow{a_ip}$.
3. If a_i belongs to the interior of an edge $e_1^i\in T_i$ and a_{i+1} is a corner of T_i not contained in e_1^i, $X_i=(a_{i+1})$, see Fig. 6c.
4. If a_i and a_{i+1} belong to the interior of two different edges $e_1^i,e_2^i\in T_i$, X_i is the common endpoint of e_1^i and e_2^i, see Fig. 6d.

Note that the four conditions in Definition 1 cover all possible cases. Thus, each shortest path $SP_w(s,t)$ corresponds to a single unique $X(s,t)$.

Let $(s=u_1,u_2,\ldots,u_\ell=t)$ be the sequence of consecutive points where $X(s,t)$ and $SP_w(s,t)$ coincide. The union of $SP_w(s,t)$ and $X(s,t)$ between two consecutive points u_j and u_{j+1}, for $1\le j<\ell$, induces a weakly simple polygon (see [12] for a formal definition). Henceforth, we use the term polygon to mean weakly simple polygon. We distinguish six different types of weakly simple polygons, denoted $P_1,\ldots,P_6$, depending on the number of edges of $\mathcal{T}$ intersected by $SP_w(u_j,u_{j+1})$, see Fig. 7.

Definition 2. Let u_j and u_{j+1} be two consecutive points where $X(s,t)$ and $SP_w(s,t)$ coincide in a triangular tessellation. Let p be a corner of $\mathcal{T}$ contained in $X(u_j,u_{j+1})$. A weakly simple polygon induced by u_j and u_{j+1} is of *type* P_k, for $1\le k\le 6$, if the subpath $SP_w(u_j,u_{j+1})$ intersects k consecutive edges around p.

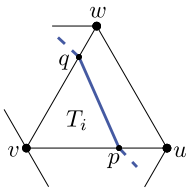

Fig. 8. Subpath of a weighted shortest path $SP_w(s,t)$ between two points p and q.

The weakly simple polygons are an important tool in our proof, since it is enough to upper-bound $\frac{\|X(s,t)\|}{\|SP_w(s,t)\|}$ for polygons of each type $P_1,\ldots,P_6$.

Lemma 1. *The polygons from Definition 2 are the only weakly simple polygons that can arise.*

Proof. Suppose the point u_j is a vertex, then if the next point where $SP_w(s,t)$ changes cell belongs to the same edge as u_j then we have a polygon of type P_1, by Definition 1, part 1. Otherwise, we obtain a polygon of type P_k, by Definition 1, parts 2 and 4.

Now, suppose u_j is a point on the interior of an edge. Let b be the next point where $SP_w(s,t)$ changes the cell(s) it belongs to. Then if b belongs to the same edge as u_j, we obtain a polygon of type P_1, by Definition 1, part 1. Otherwise, there is a set of points where $SP_w(s,t)$ coincides with k consecutive edges around a point p, which is the common endpoint of the edges containing u_j and b. Hence, by Definition 1, parts 3 and 4, $X(s,t)$ intersects u_j, p, and u_{j+1}, which is the last point of the set. Thereby, defining polygons of type $P_2,\ldots,P_6$ depending on the value of k. □

2.2. Bounding the ratio for weakly simple polygons

We are now ready to upper-bound the ratio $\frac{\|X(u_j,u_{j+1})\|}{\|SP_w(u_j,u_{j+1})\|}$ for each of the six types of weakly simple polygons in $G_{6\text{corner}}$.

First, we make a geometric observation that will be needed later. Let p and q be two points that are in the interior of two different edges on the boundary of the same triangular cell. Then, the length of the segment between p and q is given in Observation 2, which can be proved using the law of cosines.

Observation 2. *Let T_i be a triangular cell, and let (u,v,w) be the three vertices of T_i, in clockwise order. Let $p\in[u,v]$ and $q\in[v,w]$ be two points on the boundary of T_i, see Fig. 8. Then, $|pq|=\sqrt{|pv|^2+|vq|^2-|pv||vq|}$.*

We observe that, by definition, we have $\frac{\|X(u_j,u_{j+1})\|}{\|SP_w(u_j,u_{j+1})\|}=1$ for a polygon of type P_1. Therefore, our focus will be on bounding polygons of type $P_2,\ldots,P_6$. We begin from the simpler case of polygons of type $P_3,\ldots,P_6$, and later we will consider a polygon of type P_2, whose analysis is substantially more involved.

Lemma 2. *Let $u_j,\ u_{j+1}\in\mathcal{T}$ be two consecutive points where a shortest path $SP_w(s,t)$ and the crossing path $X(s,t)$ coincide. If u_j,u_{j+1} induce a weakly simple polygon of type P_k, for $3\le k\le 6$, then $\frac{\|X(u_j,u_{j+1})\|}{\|SP_w(u_j,u_{j+1})\|}\le\frac{2}{\sqrt{3}}$.*

Proof. Let $T_{i-1}\cap T_i$ be the cell boundary containing u_j, and let $T_{i+k-2}\cap T_{i+k-1}$ be the cell boundary containing u_{j+1}, see Fig. 9 for an example with $k=3$. Since u_j and u_{j+1} are two consecutive points where $SP_w(s,t)$ and $X(s,t)$ coincide, and they induce a polygon of type P_k, $SP_w(s,t)$ enters T_i from T_{i-1} through u_j, and $SP_w(s,t)$ leaves T_{i+k-2}, and enters T_{i+k-1} through u_{j+1}. Let (v_1^i,p,v_2^i) be the sequence of consecutive vertices on the boundary of T_i, in clockwise order, and $(v_1^{i+k-2},p,v_2^{i+k-2})$ be the sequence of consecutive vertices on the boundary of T_{i+k-2}, in clockwise order. Let $x\in[v_2^i,p]$ be the point where $SP_w(s,t)$ leaves T_i, and let $y\in[v_1^{i+k-2},p]$ be the point where $SP_w(s,t)$ enters T_{i+k-2}. Let a,b,c,d be the lengths $|u_jp|$, $|u_jx|$, $|u_{j+1}p|$, and $|u_{j+1}y|$, respectively.

An upper bound on the ratio $\frac{\|X(u_j,u_{j+1})\|}{\|SP_w(u_j,u_{j+1})\|}$ in a polygon of type P_k is given by

$$\frac{\|X(u_j,u_{j+1})\|}{\|SP_w(u_j,u_{j+1})\|}=\frac{a\min\{\omega_{i-1},\omega_i\}+c\min\{\omega_{i+k-2},\omega_{i+k-1}\}}{b\omega_i+\|SP_w(x,y)\|+d\omega_{i+k-2}}\le\frac{a\omega_i+c\omega_{i+k-2}}{b\omega_i+d\omega_{i+k-2}}\le$$
$$\le\frac{a\omega_i+c\omega_{i+k-2}}{\frac{\sqrt{3}}{2}a\omega_i+\frac{\sqrt{3}}{2}c\omega_{i+k-2}}=\frac{a\omega_i+c\omega_{i+k-2}}{\frac{\sqrt{3}}{2}(a\omega_i+c\omega_{i+k-2})}=\frac{2}{\sqrt{3}}.$$

Note that the $\|SP_w(x,y)\|$ term in the second denominator is zero for the case of P_3, while for $P_k, k\ge 4$, will just make the fraction smaller. Also, the last inequality comes from the fact that $[p,u_j]$ is the side of a triangle adjacent to an angle of $\frac{\pi}{3}$,

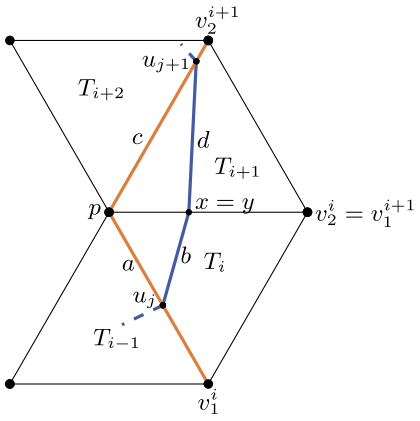

Fig. 9. Subpaths of the crossing path $X(s,t)$ (orange), and $SP_w(s,t)$ (blue) traversing a polygon of type P_3 in a triangular tessellation.

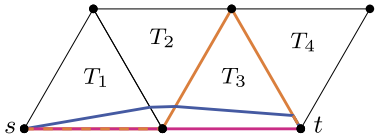

Fig. 10. The weights of the cells are $\omega_1{=}2,\ \omega_2{=}1.5,\ \omega_3{=}2$, and $\omega_4{=}1.2$. The ratio $\frac{\|X(s,t)\|}{\|SP_w(s,t)\|}$ is ≈ 1.19, whereas the ratio $\frac{\|\Pi_3(s,t)\|}{\|SP_w(s,t)\|}$ is almost 1.

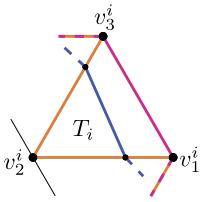

Fig. 11. Weighted shortest path $SP_w(s,t)$ (blue), crossing path $X(s,t)$ (orange), and shortcut path $\Pi_i(s,t)$ (purple) intersecting a weakly simple polygon of type P_2.

and $[u_j, x]$ is the side opposite to this angle. Hence, if we want to minimize the length of $[u_j, x]$, it has to be perpendicular to $[p, u_j]$, so $|u_j x| \geq |pu_j| \sin\frac{\pi}{3} = |pu_j|\frac{\sqrt{3}}{2}$. An analogous reasoning can be applied in triangle T_{i+1} for distances c and d. □

Next, we present a similar bound for a polygon of type P_2. There is the added difficulty that for a polygon of type P_2 it is possible to find an instance where $SP_w(s,t)$ intersects a weakly simple polygon of type P_2 such that the ratio $\frac{\|X(s,t)\|}{\|SP_w(s,t)\|}$ is much larger than $\frac{\|SGP_w(s,t)\|}{\|SP_w(s,t)\|}$, see Fig. 10. However, between s and t there are other grid paths shorter than $X(s,t)$ that intersect a polygon of type P_2. In order to obtain an upper bound when $SP_w(s,t)$ intersects a polygon of type P_2, we need a finer analysis.

In Definition 3 we define another class of grid paths, called *shortcut paths*, that gives a tighter upper bound on the ratio $\frac{\|SGP_w(s,t)\|}{\|SP_w(s,t)\|}$ when a weakly simple polygon of type P_2 is intersected by $SP_w(s,t)$. See the purple path in Fig. 11.

Definition 3. Let $SP_w(s,t)$ enter and leave cell $T_i \in \mathcal{T}$ through the edges $[v_1^i, v_2^i]$ and $[v_2^i, v_3^i]$, respectively. If $X(s,t)$ contains the subpath (v_1^i, v_2^i, v_3^i), the *shortcut path* $\Pi_i(s,t)$ is defined as the grid path $X(s, v_1^i) \cup (v_1^i, v_3^i) \cup X(v_3^i, t)$.

By using the shortcut path $\Pi_i(s,t)$, we obtain a relation between the weights of the cells adjacent to $T_i \in \mathcal{T}$ intersected by the crossing path $X(s,t)$. Before obtaining an upper bound on the ratio $\frac{\|X(s,t)\|}{\|SP_w(s,t)\|}$ for a polygon of type P_2, we define a P_2-*triple* of cells, see Fig. 12, that will be useful later.

Definition 4. A P_2-*triple* between two vertices s and t is defined as a set of five consecutive cells $T_1, \ldots, T_5$ with the following properties:

- The cells form a strip of width $\sqrt{3}$.
- s is the vertex common to T_1 and T_2 not adjacent to T_3.

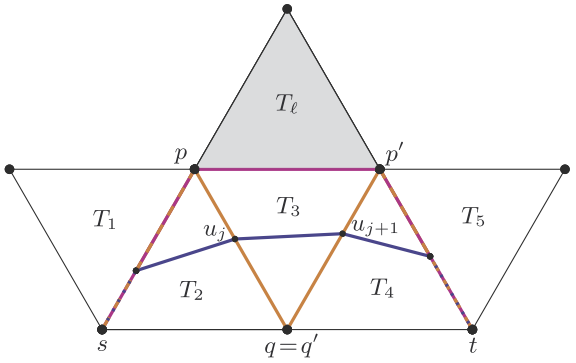

Fig. 12. P_2-triple between s and t is depicted in white. $SP_w(s,t)$, $\Pi_3(s,t)$ and $X(s,t)$ are depicted in blue, purple and orange, respectively. Observe that the three paths coincide when $SP_w(s,t)$ coincide with the edges of the cells.

- t is the vertex common to T_4 and T_5 not adjacent to T_3.
- $SP_w(s,t)$ determines three weakly simple polygons of type P_2, one around each of the vertices of T_3.

By using P_2-triples we reduce the number of cases to analyze. Using Observation 1, Lemma 2, and the definition of polygons P_1, we know that the only type of weakly simple polygon that could give a ratio larger than $\frac{2}{\sqrt{3}}$ is a P_2. Thus, we can assume that the shortest paths giving the maximum ratio intersect a weakly simple polygon P_2, and that this ratio is larger than $\frac{2}{\sqrt{3}}$ (otherwise, $\frac{\|X(s,t)\|}{\|SP_w(s,t)\|} \leq \frac{2}{\sqrt{3}}$, and we are done.).

In the following, we replace a given instance by a P_2-triple, corresponding to a weakly simple polygon of type P_2 that has the same ratio as the given instance. Thus, instead of upper-bounding the ratio of the given instance, we can do it for the P_2-triple, which is substantially easier.

Lemma 3. *For any weakly simple polygon P' of type P_2, a P_2-triple can be defined such that P' is the polygon of type P_2 of the vertex $T_2 \cap T_3 \cap T_4$, and the weights $\omega_2, \omega_3, \omega_4$ remain as in P'. We say that this P_2-triple* corresponds *to the weakly simple polygon P'.*

Proof. Let u_j and u_{j+1} be the points where $SP_w(s,t)$ respectively enters and leaves P', and let $u_j, u_{j+1} \in T_{j'}$. Consider a P_2-triple intersected by a path $SP_w(s',t')$ where the weights of the cells T_2, T_3, and T_4 are, respectively, the same as the weights of cells $T_{j'-1}$, $T_{j'}$ and $T_{j'+1}$ in the former instance. The weights of the cells T_1 and T_5 are obtained by solving the system of equations given by Snell's law of refraction. By construction, this P_2-triple is a valid instance of $SP_w(s',t')$, and it intersects the cell T_3 forming the same weakly simple polygon P' as in the former instance. □

Lemma 3 allows us to assume, from now on, that an upper bound on the ratio $\frac{\|X(s,t)\|}{\|SP_w(s,t)\|}$ is given by the length of a path that intersects a P_2-triple as in Definition 4.

Lemma 4. *Let $\frac{\|SGP_w(s,t)\|}{\|SP_w(s,t)\|}$ be the maximum ratio attained by any path intersecting a polygon of type P_2. Consider its corresponding P_2-triple. Let T_3 be the cell where the maximum ratio $\frac{\|X(u_j,u_{j+1})\|}{\|SP_w(u_j,u_{j+1})\|}$, $u_j, u_{j+1} \in T_3$ is attained. Then, $\|X(s,t)\| = \|\Pi_3(s,t)\|$.*

Proof. We prove the result by contradiction, arguing that if there is at least one grid path $GP_w(s,t)$ among $\{X(s,t), \Pi_3(s,t)\}$, that is strictly shorter than the other grid path, then this instance cannot maximize $\frac{\|SGP_w(s,t)\|}{\|SP_w(s,t)\|}$. We will show this by finding another assignment of weights w' for the cells $T_1, \ldots, T_5$, such that $\frac{\|GP_{w'}(s,t)\|}{\|SP_{w'}(s,t)\|} > \frac{\|GP_w(s,t)\|}{\|SP_w(s,t)\|}$, proving that the given instance does not provide the maximum ratio.

We first set the weight of all the cells that are not traversed by $X(s,t)$ to infinity. This way, we ensure that when modifying the weights of some cells, the combinatorial structure of the shortest path is preserved. Let T_ℓ be the cell that shares the edge of $\Pi_3(s,t)$ with T_3, see Fig. 12. Recall that ω_i is the weight of the triangular cell T_i. Then, the weighted length of the crossing path $X(s,t)$ along the edges of T_3 is $2\min\{\omega_2,\omega_3\} + 2\min\{\omega_3,\omega_4\}$, and the weighted length of the shortcut path $\Pi_3(s,t)$ along the edges of T_3 is $2\min\{\omega_3,\omega_\ell\} = 2\omega_3$ (because $\omega_\ell = \infty$). Let u_j and u_{j+1} be two consecutive points where $X(s,t)$ and $SP_w(s,t)$ coincide. Let $[p,q]$, and $[p',q']$ be, respectively, the edges containing u_j and u_{j+1}, where $p, p' \in T_\ell$.

- If $GP_w(s,t) = X(s,t)$ then $\|X(s,t)\| < \|\Pi_3(s,t)\|$, and we have that

$$\min\{\omega_2,\omega_3\} + \min\{\omega_3,\omega_4\} < \omega_3. \tag{1}$$

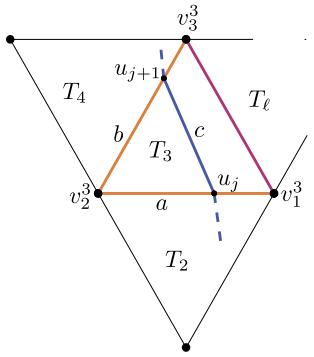

Fig. 13. Subpaths of the grid path $\Pi_3(s,t)$ (purple), the crossing path $X(s,t)$ (orange), and $SP_w(s,t)$ (blue) traversing a polygon of type P_2 in a triangular tessellation.

– If $\omega_3 \leq \omega_2$, then $\omega_3 + \min\{\omega_3, \omega_4\} < \omega_3$, which is not possible since $\min\{\omega_3, \omega_4\} \geq 0$. Hence, $\omega_3 > \omega_2$.
– If $\omega_3 \leq \omega_4$, then $\min\{\omega_2, \omega_3\} + \omega_4 < \omega_3$, which is not possible since $\min\{\omega_2, \omega_3\} \geq 0$. Hence, $\omega_3 > \omega_4$.
These two facts together with Equation (1) imply that $\omega_2 + \omega_4 < \omega_3$. We also have that

$$\frac{\|GP_w(s,t)\|}{\|SP_w(s,t)\|} = \frac{\|X(s,p)\| + 2(\omega_2+\omega_4) + \|X(p',t)\|}{\|SP_w(s,u_j)\| + |u_j u_{j+1}|\omega_3 + \|SP_w(u_{j+1},t)\|}$$

and we know that $|u_j u_{j+1}| > 0$, so we can decrease the weight ω_3, increasing the ratio.

- Otherwise, if $GP_w(s,t) = \Pi_3(s,t)$ then $\|\Pi_3(s,t)\| < \|X(s,t)\|$, and we have that $\omega_3 < \min\{\omega_2, \omega_3\} + \min\{\omega_3, \omega_4\}$. We also have that

$$\frac{\|GP_w(s,t)\|}{\|SP_w(s,t)\|} = \frac{\|\Pi_3(s,p)\| + 2\omega_3 + \|\Pi_3(p',t)\|}{\|SP_w(s,u_j)\| + \|SP_w(u_j,u_{j+1})\| + \|SP_w(u_{j+1},t)\|}.$$

The ratio $\frac{\|GP_w(s,t)\|}{\|SP_w(s,t)\|}$ is a strictly monotonic function for every ω_k [15,37]. So, if this function is decreasing in the direction of ω_3, we can decrease the weight ω_3. Otherwise, we can increase the weight ω_3. In both cases, we can increase the ratio.

Thus, we found another weight assignment w' such that $\frac{\|GP_{w'}(s,t)\|}{\|SP_{w'}(s,t)\|} > \frac{\|GP_w(s,t)\|}{\|SP_w(s,t)\|}$. In addition, the change in ω_3 can be as small as needed so that the weighted length of $GP_{w'}(s,t)$ is not larger than that of the other grid path in the set $\{X(s,t), \Pi_3(s,t)\}$ with the new weight assignment w' and, thus, it does not change which of the two grid paths in the set is the shorter one. □

Now, we have all the tools needed to obtain an upper bound on the ratio $\frac{\|X(u_j,u_{j+1})\|}{\|SP_w(u_j,u_{j+1})\|}$ for a P_2-triple. Lemma 5 presents an upper bound on this ratio where $u_j, u_{j+1} \in T_3$ are two consecutive points where $X(s,t)$ and $SP_w(s,t)$ coincide, and $\|X(s,t)\| = \|\Pi_3(s,t)\|$. Since the exact shape of $SP_w(s,t)$ is unknown, when computing the ratio in Lemma 5, we will maximize the ratio for any position of the points u_j and u_{j+1}.

Lemma 5. *Let $u_j, u_{j+1} \in T_3$, be two consecutive points where a shortest path $SP_w(s,t)$ and the crossing path $X(s,t)$ coincide. If u_j, u_{j+1} induce a weakly simple polygon of type P_2, and $\|X(s,t)\| = \|\Pi_3(s,t)\|$, then $\frac{\|X(u_j,u_{j+1})\|}{\|SP_w(u_j,u_{j+1})\|} \leq \frac{2}{\sqrt{3}}$.*

Proof. Let (v_1^3, v_2^3, v_3^3) be the sequence of vertices on the boundary of T_3 in clockwise order. Since u_j and u_{j+1} are two consecutive points where $SP_w(s,t)$ and $X(s,t)$ coincide, and they induce a polygon of type P_2, $SP_w(s,t)$ enters T_3 from cell T_2 through u_j, and $SP_w(s,t)$ leaves T_3 and enters cell T_4 through u_{j+1}, see Fig. 13. Suppose, without loss of generality, that $u_j \in [v_1^3, v_2^3]$ and $u_{j+1} \in [v_2^3, v_3^3]$. Let a, b, c be the lengths $|u_j v_2^3|$, $|v_2^3 u_{j+1}|$, and $|u_j u_{j+1}|$, respectively. According to Observation 2, $c = \sqrt{a^2 + b^2 - ab}$. We want to maximize the ratio $\frac{\|X(u_j,u_{j+1})\|}{\|SP_w(u_j,u_{j+1})\|}$ for all weight assignments of ω_2, ω_3, and ω_4.

Traversing cell T_3 there is also the grid path $\Pi_3(s,t)$. Let T_ℓ be the cell that shares the edge of $\Pi_3(s,t)$ with T_3. Since $\|X(s,t)\| = \|\Pi_3(s,t)\|$, $2\min\{\omega_2, \omega_3\} + 2\min\{\omega_3, \omega_4\} = 2\min\{\omega_3, \omega_\ell\}$. Thus, we distinguish two cases: $b \leq a$ and $b > a$. In the first case we take:

$$\min\{\omega_2, \omega_3\} = \min\{\omega_3, \omega_\ell\} - \min\{\omega_3, \omega_4\}.$$

In the second case we take:

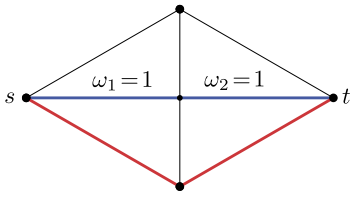

Fig. 14. $SP_w(s,t)$ and $SGP_w(s,t)$ are depicted in blue and red, respectively. The ratio $\frac{\|SGP_w(s,t)\|}{\|SP_w(s,t)\|}$ is $\frac{2}{\sqrt{3}}$.

$$\min\{\omega_3, \omega_4\} = \min\{\omega_3, \omega_\ell\} - \min\{\omega_2, \omega_3\}.$$

Then, an upper bound on the ratio $R = \frac{\|X(u_j,u_{j+1})\|}{\|SP_w(u_j,u_{j+1})\|}$ in a polygon of type P_2 is:

$$R = \frac{a\min\{\omega_2,\omega_3\} + b\min\{\omega_3,\omega_4\}}{c\omega_3} \leq \begin{cases} \overbrace{\leq}^{\text{if } b\leq a} \frac{a\min\{\omega_3,\omega_\ell\}+(b-a)\min\{\omega_3,\omega_4\}}{c\omega_3} \leq \\ \overbrace{\leq}^{\text{if } a<b} \frac{b\min\{\omega_3,\omega_\ell\}+(a-b)\min\{\omega_2,\omega_3\}}{c\omega_3} \leq \end{cases}$$

$$\leq \begin{cases} \frac{a\min\{\omega_3,\omega_\ell\}}{c\omega_3} \leq \frac{a}{\sqrt{a^2+b^2-ab}} \\ \frac{b\min\{\omega_3,\omega_\ell\}}{c\omega_3} \leq \frac{b}{\sqrt{a^2+b^2-ab}} \end{cases} \leq \frac{2}{\sqrt{3}},$$

where the last inequality in the two ratios is obtained by maximization over the values of $a \in [0,2]$ and $b \in [0,2]$. □

Finally, we have all the pieces to prove our main result.

Theorem 1. *In $G_{6corner}$, $\frac{\|SGP_w(s,t)\|}{\|SP_w(s,t)\|} \leq \frac{2}{\sqrt{3}}$.*

Proof. Let $SP_w(s,t)$ be a weighted shortest path between two corners s and t in a triangular tessellation. Let $X(s,t)$ be the crossing path from s to t obtained from $SP_w(s,t)$. By Observation 1, $\frac{\|X(s,t)\|}{\|SP_w(s,t)\|} \leq \frac{\|X(u_j,u_{j+1})\|}{\|SP_w(u_j,u_{j+1})\|}$, over all pairs (u_j, u_{j+1}) of consecutive points where $SP_w(s,t)$ and $X(s,t)$ coincide.

As already observed, the ratio $\frac{\|X(u_j,u_{j+1})\|}{\|SP_w(u_j,u_{j+1})\|}$ is 1 in a polygon of type P_1. Further, by Lemma 2, that ratio is at most $\frac{2}{\sqrt{3}}$ for weakly simple polygons of type P_k, $k > 2$. Finally, using Lemmas 3 and 4, we know that if a path intersecting cell T_3 is the path that maximizes the ratio $\frac{\|X(u_j,u_{j+1})\|}{\|SP_w(u_j,u_{j+1})\|}$ in a weakly simple polygon of type P_2, then $\|X(s,t)\| = \|\Pi_3(s,t)\|$. And, in this case, by Lemma 5 we get that the ratio $\frac{\|X(u_j,u_{j+1})\|}{\|SP_w(u_j,u_{j+1})\|}$ is at most $\frac{2}{\sqrt{3}}$, where $u_j, u_{j+1} \in T_3$.

All this implies that $\frac{\|X(s,t)\|}{\|SP_w(s,t)\|}$ is at most $\frac{2}{\sqrt{3}}$. Since $\|SGP_w(s,t)\| \leq \|X(s,t)\|$, we have that $\frac{\|SGP_w(s,t)\|}{\|SP_w(s,t)\|} \leq \frac{2}{\sqrt{3}}$. □

Fig. 14 provides an illustration of the lower bound $\frac{2}{\sqrt{3}}$ on the ratio between the weighted shortest grid path $SGP_w(s,t)$ (red) and the weighted shortest path $SP_w(s,t)$ (blue) claimed by Nash [33]. Hence, the upper bound in Theorem 1 is tight for $G_{6\text{corner}}$.

3. Ratios $\frac{\|SGP_w(s,t)\|}{\|SVP_w(s,t)\|}$ in $G_{6\text{corner}}$ and $\frac{\|SVP_w(s,t)\|}{\|SP_w(s,t)\|}$ in G_{corner}

In this section we provide results for the ratios where the weighted shortest vertex path $SVP_w(s,t)$ is involved, i.e., $\frac{\|SGP_w(s,t)\|}{\|SVP_w(s,t)\|}$ and $\frac{\|SVP_w(s,t)\|}{\|SP_w(s,t)\|}$. The length of a weighted shortest vertex path $SVP_w(s,t)$ is an upper bound for the length of a weighted shortest path $SP_w(s,t)$, so the upper bound on the ratio $\frac{\|SGP_w(s,t)\|}{\|SP_w(s,t)\|}$ obtained in Theorem 1 is an upper bound for $\frac{\|SGP_w(s,t)\|}{\|SVP_w(s,t)\|}$.

Corollary 1. *In $G_{6corner}$, $\frac{\|SGP_w(s,t)\|}{\|SVP_w(s,t)\|} \leq \frac{2}{\sqrt{3}}$.*

When the weights of the cells are in the set $\{1, \infty\}$, the ratio $\frac{\|SGP_w(s,t)\|}{\|SVP_w(s,t)\|}$ was proved to be at most $\frac{2}{\sqrt{3}}$ by Nash [33]. In addition, Nash showed that this bound is tight. Thus, for general (non-negative) weights this value is a lower bound on the ratio $\frac{\|SGP_w(s,t)\|}{\|SVP_w(s,t)\|}$ for $G_{6\text{corner}}$.

As a corollary of Theorem 1, we obtain Corollary 2. The result comes from the fact that $\|SVP_w(s,t)\|$ is a lower bound for $\|SGP_w(s,t)\|$. Recall that $SVP_w(s,t)$ and $SP_w(s,t)$ do not use $G_{6\text{corner}}$, but G_{corner}.

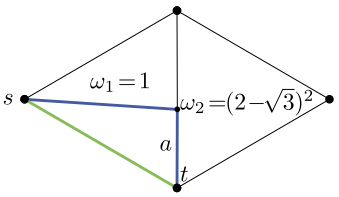

Fig. 15. $SP_w(s,t)$ and $SVP_w(s,t)$ are depicted in blue and green, respectively. The ratio $\frac{\|SVP_w(s,t)\|}{\|SP_w(s,t)\|}$ is $\frac{2\sqrt{7\sqrt{3}-12}}{(7-4\sqrt{3})(6\sqrt{2}+\sqrt{7\sqrt{3}-12})}$ when $a = \frac{4-(4\sqrt{6}+7\sqrt{2})\sqrt{1351\sqrt{3}-2340}}{4} \approx 0.87$.

Corollary 2. *In* G_{corner}, $\frac{\|SVP_w(s,t)\|}{\|SP_w(s,t)\|} \leq \frac{2}{\sqrt{3}} \approx 1.15$.

Finally, we provide a lower bound for the ratio $\frac{\|SVP_w(s,t)\|}{\|SP_w(s,t)\|}$. The green path in Fig. 15 is a weighted shortest vertex path $SVP_w(s,t)$ between vertices s and t, thus, we have the following result.

Observation 3. *In* G_{corner}, $\frac{\|SVP_w(s,t)\|}{\|SP_w(s,t)\|} \geq \frac{2\sqrt{7\sqrt{3}-12}}{(7-4\sqrt{3})(6\sqrt{2}+\sqrt{7\sqrt{3}-12})} \approx 1.11$.

4. Discussion and future work

We presented bounds on the ratio between the lengths of three types of weighted shortest paths in a triangular tessellation. The fact that a compact grid graph such as $G_{6\text{corner}}$ guarantees an error bound of $\approx 15\%$, regardless of weights used, justifies its widespread use in applications in areas such as gaming and simulation, where performance is a priority over accuracy.

Our analysis techniques, presented here for triangular grids, can also be applied to obtain upper bounds for the same ratios in the other two types of regular tessellations, square and hexagonal. In particular, we recently proved upper bounds of $R = \frac{2}{\sqrt{2+\sqrt{2}}}$ for weighted square cells [9], and $R = \frac{3}{2}$ when we only allow movement along the edges of an hexagonal tessellation [8]. The main differences lie in the exact definition of the crossing paths and the weakly simple polygons. Our techniques can also be used to derive upper bounds for another type of grid graph, where the vertices are cell centers instead of corners (see, e.g., [7,24,33]).

For future work, it would be interesting to close the gap for $\frac{\|SVP_w(s,t)\|}{\|SP_w(s,t)\|}$, of approximately 0.04. It is an intriguing question whether the seemingly richer any-angle path $SVP_w(s,t)$ can actually guarantee a better quality factor than $G_{6\text{corner}}$. However, our results show that, even if that is the case, the improvement is rather negligible.

Declaration of competing interest

The authors declare that they have no known competing financial interests or personal relationships that could have appeared to influence the work reported in this paper.

Data availability

No data was used for the research described in the article.

Acknowledgements

P. B. is partially supported by NSERC. G. E., D. O. and R. I. S. are partially supported by H2020-MSCA-RISE project 734922 - CONNECT and project PID2019-104129GB-I00 funded by MCIN/AEI/10.13039/501100011033. G. E. and D. O. are also supported by PIUAH21/IA-062 and CM/JIN/2021-004. G. E. is also funded by an FPU of the Universidad de Alcalá.

The authors want to thank Vsevolod Kvachev for granting permission to use the screenshots of the game "Colossal Citadels".

The authors thank the anonymous referees for their comments and insights which greatly improved the readability of this article.

References

[1] L. Aleksandrov, M. Lanthier, A. Maheshwari, J.R. Sack, An ε-approximation algorithm for weighted shortest paths on polyhedral surfaces, in: Scandinavian Workshop on Algorithm Theory, Springer, 1998, pp. 11–22.

[2] L. Aleksandrov, A. Maheshwari, J.R. Sack, Approximation algorithms for geometric shortest path problems, in: Proceedings of the Thirty-Second Annual ACM Symposium on Theory of Computing, 2000, pp. 286–295.

[3] L. Aleksandrov, A. Maheshwari, J.R. Sack, Determining approximate shortest paths on weighted polyhedral surfaces, J. ACM 52 (1) (2005) 25–53.
[4] A. Ammar, H. Bennaceur, I. Chăari, A. Koubăa, M. Alajlan, Relaxed Dijkstra and A^* with linear complexity for robot path planning problems in large-scale grid environments, Soft Comput. 20 (10) (2016) 4149–4171.
[5] D. Bachmann, F. Bökler, J. Kopec, K. Popp, B. Schwarze, F. Weichert, Multi-objective optimisation based planning of power-line grid expansions, ISPRS Int.l J. Geo-Inf. 7 (7) (2018) 258.
[6] J.P. Bailey, A. Nash, C.A. Tovey, S. Koenig, Path-length analysis for grid-based path planning, Artif. Intell. 301 (2021) 103560.
[7] J.P. Bailey, C. Tovey, T. Uras, S. Koenig, A. Nash, Path planning on grids: the effect of vertex placement on path length, in: Eleventh Artificial Intelligence and Interactive Digital Entertainment Conference, 2015.
[8] P. Bose, G. Esteban, D. Orden, R.I. Silveira, On approximating shortest paths in weighted hexagonal tessellations, in: Abstracts of the Computational Geometry: Young Researchers Forum 2022 (CG:YRF), 2022, pp. 27–31.
[9] P. Bose, G. Esteban, D. Orden, R.I. Silveira, Spanning ratio of shortest paths in weighted square tessellations, in: Abstracts of the 38th European Workshop on Computational Geometry (EuroCG), vol. 65, 2022, pp. 1–8.
[10] J. Carsten, D. Ferguson, A. Stentz, 3D field D^*: improved path planning and replanning in three dimensions, in: 2006 IEEE/RSJ International Conference on Intelligent Robots and Systems, IEEE, 2006, pp. 3381–3386.
[11] J. Carsten, A. Rankin, D. Ferguson, A. Stentz, Global planning on the Mars exploration rovers: software integration and surface testing, J. Field Robot. 26 (4) (2009) 337–357.
[12] H.C. Chang, J. Erickson, C. Xu, Detecting weakly simple polygons, in: Proceedings of the Twenty-Sixth Annual ACM-SIAM Symposium on Discrete Algorithms, SIAM, 2014, pp. 1655–1670.
[13] D.Z. Chen, K.S. Klenk, H.Y. Tu, Shortest path queries among weighted obstacles in the rectilinear plane, SIAM J. Comput. 29 (4) (2000) 1223–1246.
[14] S.W. Cheng, J. Jin, A. Vigneron, Triangulation refinement and approximate shortest paths in weighted regions, in: P. Indyk (Ed.), Proceedings of the Twenty-Sixth Annual ACM-SIAM Symposium on Discrete Algorithms, SODA 2015, San Diego, CA, USA, January 4-6, 2015, SIAM, 2015, pp. 1626–1640.
[15] K.L. Chew, E.U. Choo, Pseudolinearity and efficiency, Math. Program. 28 (2) (1984) 226–239.
[16] J.L. de Carufel, C. Grimm, A. Maheshwari, M. Owen, M. Smid, A note on the unsolvability of the weighted region shortest path problem, Comput. Geom. 47 (7) (2014) 724–727.
[17] L. de Floriani, P. Magillo, E. Puppo, Applications of computational geometry to geographic information systems, in: Handbook of Computational Geometry, vol. 7, 2000, pp. 333–388.
[18] M. Garcia, A. Viguria, A. Ollero, Dynamic graph-search algorithm for global path planning in presence of hazardous weather, J. Intell. Robot. Syst. 69 (1) (2013) 285–295.
[19] D. Gaw, A. Meystel, Minimum-time navigation of an unmanned mobile robot in a 2-1/2D world with obstacles, in: Proceedings of the 1986 IEEE International Conference on Robotics and Automation, vol. 3, IEEE, 1986, pp. 1670–1677.
[20] L. Gewali, A.C. Meng, J.S.B. Mitchell, S.C. Ntafos, Path planning in $0/1/\infty$ weighted regions with applications, INFORMS J. Comput. 2 (3) (1990) 253–272.
[21] F. Hanssen, R. May, J. Thomassen, K. Bevanger, A least cost path (LCP) toolbox for optimal routing of high voltage power lines for a sustainable future, in: 10th Int. Symp. Environmental Concerns in Rights-of-Way Management, USA Utility Arborist Association Champaign, IL, 2014, pp. 181–186.
[22] D.D. Harabor, A. Grastien, D. Öz, V. Aksakalli, Optimal any-angle pathfinding in practice, J. Artif. Intell. Res. 56 (2016) 89–118.
[23] P.C. Hew, The length of shortest vertex paths in binary occupancy grids compared to shortest r-constrained ones, J. Artif. Intell. Res. 59 (2017) 543–563.
[24] N.S. Jaklin, On Weighted Regions and Social Crowds: Autonomous-agent Navigation in Virtual Worlds, PhD thesis, Utrecht University, 2016.
[25] A. Kamphuis, M. Rook, M.H. Overmars, Tactical path finding in urban environments, in: First International Workshop on Crowd Simulation, Citeseer, 2005.
[26] Konami, Metal Gear, PC, NES, Mobile phone, 1987.
[27] B. Kramm, N. Rivera, C. Hernández, J.A. Baier, A suboptimality bound for 2^k grid path planning, in: Eleventh Annual Symposium on Combinatorial Search, 2018.
[28] V. Kvachev, Colossal citadels, http://colossalcitadels.com. (Accessed 5 April 2022).
[29] J. Li, D. Harabor, P.J. Stuckey, H. Ma, G. Gange, S. Koenig, Pairwise symmetry reasoning for multi-agent path finding search, Artif. Intell. 301 (2021) 103574.
[30] J.S.B. Mitchell, An algorithmic approach to some problems in terrain navigation, Artif. Intell. 37 (1–3) (1988) 171–201.
[31] J.S.B. Mitchell, C. Papadimitrou, The weighted region problem: finding shortest paths through a weighted planar subdivision, J. ACM 38 (1) (1991) 18–73.
[32] B.N. Nagy, Shortest paths in triangular grids with neighbourhood sequences, Int. J. Comput. Inf. Technol. 11 (2) (2003) 111–122.
[33] A. Nash, Any-Angle Path Planning, PhD thesis, University of Southern California, 2012.
[34] A. Nash, K. Daniel, S. Koenig, A. Felner, Theta*: any-angle path planning on grids, in: AAAI, vol. 7, 2007, pp. 1177–1183.
[35] P. Papadakis, Terrain traversability analysis methods for unmanned ground vehicles: a survey, Eng. Appl. Artif. Intell. 26 (4) (2013) 1373–1385.
[36] N. Piveteau, J. Schito, M. Raubal, R. Weibel, A novel approach to the routing problem of overhead transmission lines, PhD thesis, Geographisches Institut der Universität Zürich, 2017.
[37] T. Rapcsák, On pseudolinear functions, Eur. J. Oper. Res. 50 (3) (1991) 353–360.
[38] N.C. Rowe, R.S. Ross, Optimal grid-free path planning across arbitrarily contoured terrain with anisotropic friction and gravity effects, IEEE Trans. Robot. Autom. 6 (5) (1990) 540–553.
[39] A.H.M. Santos, R.M. de Lima, C.R.S. Pereira, R. Osis, G.O.S. Medeiros, A.R. de Queiroz, B.K. Flauzino, A.R.P.C. Cardoso, L.C. Junior, R.A. dos Santos, et al., Optimizing routing and tower spotting of electricity transmission lines: an integration of geographical data and engineering aspects into decision-making, Electr. Power Syst. Res. 176 (2019) 105953.
[40] L. Seegmiller, T. Shirabe, C.D. Tomlin, A method for finding least-cost corridors with reduced distortion in raster space, Int. J. Geogr. Inf. Sci. 35 (8) (2021) 1570–1591.
[41] M. Sharir, S. Sifrony, Coordinated motion planning for two independent robots, Ann. Math. Artif. Intell. 3 (1) (1991) 107–130.
[42] B. Shen, M.A. Cheema, D.D. Harabor, P.J. Stuckey, Fast optimal and bounded suboptimal Euclidean pathfinding, Artif. Intell. 302 (2022) 103624.
[43] N.R. Sturtevant, D. Sigurdson, B. Taylor, T. Gibson, Pathfinding and abstraction with dynamic terrain costs, in: Proceedings of the AAAI Conference on Artificial Intelligence and Interactive Digital Entertainment, vol. 15, 2019, pp. 80–86.
[44] N. Tran, M.J. Dinneen, S. Linz, Computing close to optimal weighted shortest paths in practice, in: Proceedings of the International Conference on Automated Planning and Scheduling, vol. 30, 2020, pp. 291–299.
[45] Ubisoft Montreal, Assassin's Creed, PC, Mac, Xbox 360, PlayStation 3, 2007.
[46] W. van Toll, R. Triesscheijn, M. Kallmann, R. Oliva, N. Pelechano, J. Pettré, R. Geraerts, A comparative study of navigation meshes, in: Proceedings of the 9th International Conference on Motion in Games, 2016, pp. 91–100.
[47] G. Wagner, H. Choset, Subdimensional expansion for multirobot path planning, Artif. Intell. 219 (2015) 1–24.
[48] P.K.Y. Yap, N. Burch, R.C. Holte, J. Schaeffer, Any-angle path planning for computer games, in: Seventh Artificial Intelligence and Interactive Digital Entertainment Conference, 2011.